BLOOD FLOW THROUGH A CURVED ARTERY

G. PONTRELLI

IAC-CNR,
Viale del Policlinico, 137
00161 Roma, Italy
E-mail: g.pontrelli@iac.cnr.it

A. TATONE

DISAT, Facoltà di Ingegneria
University of L'Aquila
67040 Monteluco di Roio (AQ), Italy
E-mail: tatone@ing.univaq.it

Blood flow in a curved artery is described as the motion of a viscous fluid through a curved thin-walled elastic tube. Under the hypothesis of small curvature, an asymptotic analysis is carried out to solve the governing unsteady 3D equations. The model results an extension of the Womersley's theory for the straight elastic tube. A numerical solution is found for the first order approximation and computational results are finally presented, demonstrating the role of curvature in the wave propagation and in the development of a secondary flow.

1. Introduction

The unsteady flow of a viscous fluid in curved conduits is relevant for several applications, particularly in vascular fluid dynamics. Most of the arteries are moderately curved and blood flow through them is affected by centrifugal forces which tend to set up secondary flows, recirculating fluid vortices and cause a non symmetric distribution of the pressure and of the wall shear stress[1,2]. However, little attention has been given to address the effect of the curvature on all the components of the flow velocity and on the pressure field. Another relevant aspect of the curvature is the influence on wall shear stresses in relation to atherosclerotic diseases and the examination of time varying flow rates[3].

The steady flow in a toroidal rigid tube has been the object of a thorough investigation by Dean[4]. Most of the literature on flows in curved tubes refer to such a basic work and concern various extensions to the unsteady case,

2

but all are confined to rigid wall conduits[5,6,7]. On the other hand, when considering physiological applications, wall compliance and its interaction with the fluid constitute essential aspects that cannot be disregarded. The classical works of Womersley[8] shed light on the flow through an elastic straight tube and opened a series of following studies on the characteristics of the wave propagation in arteries[9,10,11,12,13,14]. The present work extends the theory of Womersley, recasting the flow in a curved tube as a small correction of that in a straight one. The formulation is based on the principles of fluid and solid mechanics and, under general and realistic assumptions, a formal complete procedure is described to get the final form of the fluid-wall interaction model equations. In a wave propagation context, the dependence of the model on four independent parameters is outlined: the pressure amplitude, the pulse frequency, the elasticity modulus and the curvature ratio. In particular, through a number of numerical experiments, the role of the latter is highlighted, and the character of the secondary flow addressed[15].

2. Fluid-structure interaction

The motion of blood in a bended vessel is modelled by the flow of a viscous fluid in a curved elastic tube, with the geometry of a torus. This is assumed to have a planar axis, a circular cross section of radius a and a constant radius of curvature R. An incompressible newtonian fluid of viscosity μ and density ρ is flowing within. The dynamics induced by the wall deformability modifies the fluid domain and its boundary conditions, and conversely, the flow field, through the stress exerted on the wall, induces the wall deformation (*fluid-structure interaction*). Let us first model both the fluid and the solid continuum systems with the mechanical conservation laws.

The fluid motion is given by the Navier-Stokes equation:

$$\rho \left(\frac{\partial \boldsymbol{v}}{\partial t} + \boldsymbol{v} \cdot \nabla \boldsymbol{v} \right) = -\nabla p + \mu \Delta \boldsymbol{v} \tag{1}$$

with $\boldsymbol{v}$ the velocity and p the transmural pressure. The fluid incompressibility reads as:

$$div \, \boldsymbol{v} = 0 \tag{2}$$

To model the vessel wall motion, we shall assume this is made of a thin shell of a small thickness $h \ll a$ and the theory of membranes is used to
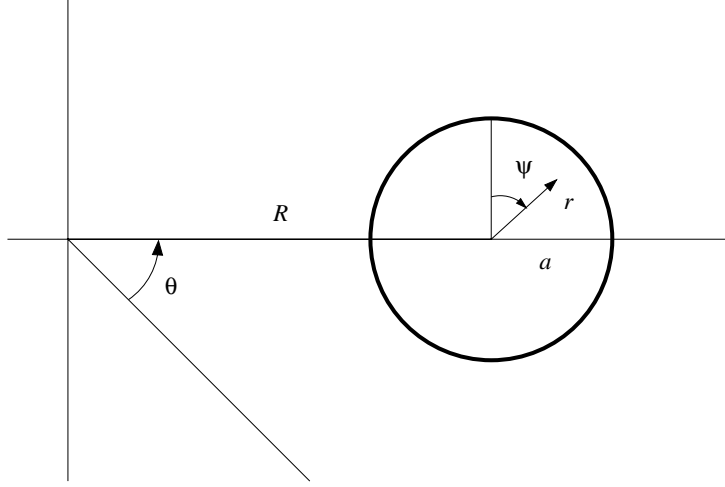
Figure 1.   Cross section of the tube (inner wall at the left, outer wall at the right) and toroidal coordinates (r, ψ, θ).

approximate it. For an elastic solid subject to external forces, the balance equation is[16]:

$$div\boldsymbol{S} = p \cdot \boldsymbol{n} - 2\mu \boldsymbol{D} \cdot \boldsymbol{n} - \rho_t \ddot{\boldsymbol{u}} \qquad (3)$$

where $\boldsymbol{S}$ is the membrane stress tensor, $\boldsymbol{D}$ is the deformation gradient, $\boldsymbol{u}$ the wall displacement and ρ_t the wall density. Owing to the small wall deformations, the membrane stress tensor $\boldsymbol{S}$ is expressed as a linear function of the strain tensor $\boldsymbol{E}$:

$$\boldsymbol{S} = \begin{pmatrix} hB\left(\epsilon_{\theta\theta} + \sigma\epsilon_{\psi\psi}\right) & 2hG\,\epsilon_{\theta\psi} \\ \\ 2hG\,\epsilon_{\theta\psi} & hB\left(\epsilon_{\psi\psi} + \sigma\epsilon_{\theta\theta}\right) \end{pmatrix} \qquad (4)$$

where E is the modulus of elasticity, σ is Poisson's ratio, $B = \dfrac{E}{1 - \sigma^2}$ and $G = \dfrac{E}{2(1 + \sigma)}$ the shear modulus[16].

Matching between fluid and wall velocities is imposed as interface fluid-wall condition:

$$\boldsymbol{v} = \dot{\boldsymbol{u}} \qquad (5)$$

Because of the geometry of the problem, it is convenient to express the fluid and wall equation in a toroidal coordinate system (r, θ, ψ) (see fig. 1).

4

We denote by $\boldsymbol{v} = (u, v, w)$ the radial (r), the tangential (ψ) and the axial (θ) components of the fluid velocity, and by $\boldsymbol{u} = (\eta, \xi, \zeta)$ the correspondent components of the wall displacement.

3. Wave solution

The steady flow in a curved rigid tube has been analyzed by Dean who found an analytical solution[4]. He used a perturbation approach based on the curvature parameter $\varepsilon = \dfrac{a}{R}$, which is supposed to be small, such that the solution up to the first order is $\bar{\chi} = \bar{\chi}_0 + \varepsilon \bar{\chi}_1$, being $\bar{\chi}_0$ the steady state solution in a straight rigid tube (Hagen-Poiseuille flow), and $\bar{\chi}_1$ is the correction due to the curvature[a]. It is well known that the vascular flow can be decomposed in a steady dominant part and, due to the wall compliance, in a small oscillatory component over it[3]. As a consequence, it is reasonable to look for a solution made up of a wave (*unsteady* component) superimposed on the previous steady solution, namely:

$$\chi = \bar{\chi}(r, \psi) + \tilde{\chi}(r, \psi) e^{i(\omega t - kz)} \tag{6}$$

where ω is the circular frequency, k the wave number (consequently $c = \dfrac{\omega}{Re(k)}$ is the wave speed) and $z = R\,\theta$ a curvilinear axial coordinate.

To simplify the mathematical problem, let us assume the unsteady solution is *small* enough such that the the response of the system can be linearized, with respect to the wave amplitudes, over the steady state solution. By means of some additional hypothesis on the wave characteristics, a further simplification concerning the relative magnitudes of some diffusive terms is made[13]. The final equations are:

Continuity equation:

$$\frac{\partial u}{\partial r} + \frac{u}{r} + \frac{1}{r} \frac{\partial v}{\partial \psi} + \frac{u \sin \psi}{R + r \sin \psi} + \frac{v \cos \psi}{R + r \sin \psi} + \frac{R}{R + r \sin \psi} \frac{\partial w}{\partial z} = 0 \quad (7)$$

Flow equations:

$$\rho \left(\frac{\partial u}{\partial t} - \frac{2\bar{w}w \sin \psi}{R + r \sin \psi} \right) = -\frac{\partial p}{\partial r} + \mu \left(\frac{\partial^2 u}{\partial r^2} + \frac{1}{r} \frac{\partial u}{\partial r} + \frac{1}{r^2} \frac{\partial^2 u}{\partial \psi^2} + \frac{\sin \psi}{R + r \sin \psi} \frac{\partial u}{\partial r} \right.$$
$$+ \frac{\cos \psi}{r\,(R + r \sin \psi)} \frac{\partial u}{\partial \psi} - \frac{u}{r^2} - \frac{2}{r^2} \frac{\partial v}{\partial \psi} - \frac{vR \cos \psi}{r\,(R + r \sin \psi)^2} - \frac{2R \sin \psi}{(R + r \sin \psi)^2} \frac{\partial w}{\partial z}$$
$$\left. - \frac{u\,\sin^2 \psi}{(R + r \sin \psi)^2} - \frac{2v\,\sin \psi \cos \psi}{(R + r \sin \psi)^2} \right) \tag{8}$$

---

[a]χ denotes the global solution of the fluid-structure interaction problem.

$$\rho \left(\frac{\partial v}{\partial t} - \frac{2\bar{w}w \cos\psi}{R + r\sin\psi} \right) = -\frac{1}{r}\frac{\partial p}{\partial \psi} + \mu \left(\frac{\partial^2 v}{\partial r^2} + \frac{1}{r}\frac{\partial v}{\partial r} + \frac{1}{r^2}\frac{\partial^2 v}{\partial \psi^2} + \frac{2}{r^2}\frac{\partial u}{\partial \psi} \right.$$
$$+ \frac{uR\cos\psi}{r\left(R + r\sin\psi\right)^2} + \frac{\sin\psi}{R + r\sin\psi}\frac{\partial v}{\partial r} + \frac{\cos\psi}{r\left(R + r\sin\psi\right)}\frac{\partial v}{\partial \psi} - \frac{v}{r^2}$$
$$\left. - \frac{2R\cos\psi}{\left(R + r\sin\psi\right)^2}\frac{\partial w}{\partial z} - \frac{v\,\cos^2\psi}{\left(R + r\sin\psi\right)^2} \right) \tag{9}$$

$$\rho\frac{\partial w}{\partial t} = -\frac{R}{R + r\sin\psi}\frac{\partial p}{\partial z} + \mu \left(\frac{\partial^2 w}{\partial r^2} + \frac{1}{r}\frac{\partial w}{\partial r} + \frac{1}{r^2}\frac{\partial^2 w}{\partial \psi^2} + \frac{\sin\psi}{R + r\sin\psi}\frac{\partial w}{\partial r} \right.$$
$$\left. + \frac{\cos\psi}{r\left(R + r\sin\psi\right)}\frac{\partial w}{\partial \psi} - \frac{w}{\left(R + r\sin\psi\right)^2} \right) \tag{10}$$

Wall equations:

$$\rho_t h \frac{\partial^2 \eta}{\partial t^2} = \left[p - 2\mu\frac{\partial u}{\partial r} \right]_{r=a} - hB \left[\frac{\eta + \dfrac{\partial \xi}{\partial \psi}}{a^2} + \frac{\sin\psi\left(\eta\sin\psi + \xi\cos\psi + R\dfrac{\partial \zeta}{\partial z}\right)}{(R + a\sin\psi)^2} \right]$$
$$- \sigma hB \left[\frac{\sin\psi\left(2\eta + \dfrac{\partial \xi}{\partial \psi}\right) + \xi\cos\psi + R\dfrac{\partial \zeta}{\partial z}}{a(R + a\sin\psi)} \right] \tag{11}$$

$$\rho_t h \frac{\partial^2 \xi}{\partial t^2} = -\mu \left[\frac{1}{r}\frac{\partial u}{\partial \psi} - \frac{v}{r} + \frac{\partial v}{\partial r} \right]_{r=a} + hB \left[\frac{\dfrac{\partial \eta}{\partial \psi} + \dfrac{\partial^2 \xi}{\partial \psi^2}}{a^2} + \cos\psi \left(\frac{\eta + \dfrac{\partial \xi}{\partial \psi}}{a(R + a\sin\psi)} \right. \right.$$
$$\left. \left. - \frac{\eta\sin\psi + \xi\cos\psi + R\dfrac{\partial \zeta}{\partial z}}{(R + a\sin\psi)^2} \right) \right] + \sigma hB \left[\frac{-\xi\sin\psi + \sin\psi\dfrac{\partial \eta}{\partial \psi} + R\dfrac{\partial^2 \zeta}{\partial \psi \partial z}}{a(R + a\sin\psi)} \right]$$
$$+ hG \left[\frac{R\dfrac{\partial^2 \zeta}{\partial z \partial \psi}}{a(R + a\sin\psi)} + \frac{R^2\dfrac{\partial^2 \xi}{\partial z^2} - R\cos\psi\dfrac{\partial \zeta}{\partial z}}{(R + a\sin\psi)^2} \right] \tag{12}$$

6

$$\rho_t h \frac{\partial^2 \zeta}{\partial t^2} = -\mu \left[\frac{R}{R + a \sin \psi} \frac{\partial u}{\partial z} - \frac{w \sin \psi}{R + a \sin \psi} + \frac{\partial w}{\partial r} \right]_{r=a}$$

$$+ hB \left[\frac{R \sin \psi \frac{\partial \eta}{\partial z} + R \cos \psi \frac{\partial \xi}{\partial z} + R^2 \frac{\partial^2 \zeta}{\partial z^2}}{(R + a \sin \psi)^2} \right] + \sigma hB \left[\frac{R \frac{\partial \eta}{\partial z} + R \frac{\partial^2 \xi}{\partial \psi \partial z}}{a(R + a \sin \psi)} \right]$$

$$+ hG \left[\frac{1}{a^2} \frac{\partial^2 \zeta}{\partial \psi^2} + \frac{R \frac{\partial^2 \xi}{\partial \psi \partial z} + \zeta \sin \psi + \cos \psi \frac{\partial \zeta}{\partial \psi}}{a(R + a \sin \psi)} + \frac{R \cos \psi \frac{\partial \xi}{\partial z} - \zeta \cos^2 \psi}{(R + a \sin \psi)^2} \right] \quad (13)$$

Interface conditions:

$$\frac{\partial \eta}{\partial t} = u \bigg|_{r=a} \qquad\qquad \frac{\partial \xi}{\partial t} = v \bigg|_{r=a} \qquad\qquad \frac{\partial \zeta}{\partial t} = w \bigg|_{r=a} \qquad (14)$$

4. Asymptotic analysis

A perturbation method is used to study the influence of a moderate curvature with respect to the straight case. First of all, the governing equations are written in terms of a normalized radial variable $y = \frac{r}{a}$ ($0 \le y \le 1$). As the curvature parameter $\varepsilon = \frac{a}{R}$ is assumed to be small ($\ll 1$), the tilded quantities $\tilde{\chi}$ (amplitudes) in Eqs. (6) are expanded as a power series of ε over an axisymmetric solution $\chi_0(y)$. By omitting $\sim$sign at the right hand side, we have:

$$\tilde{\chi}(y, \psi) = \chi_0(y) + \varepsilon \chi_1(y, \psi) + \varepsilon^2 \chi_2(y, \psi) + \dots \qquad (15)$$

The series Eq. (15) is substituted in the fluid and wall governing equations, and terms of the same power of ε, up to the first order, are equated.

   In the asymptotic expansion Eq. (15), χ_0 corresponds to the axisymmetric solution in a straight elastic tube (Womersley solution)[8]. By equating the 1st order terms in the governing Eqs. and separating the variables as follows:

$$u_1 = \hat{u}_1(y) \sin \psi \qquad v_1 = \hat{v}_1(y) \cos \psi \qquad w_1 = \hat{w}_1(y) \sin \psi$$

$$p_1 = \hat{p}_1(y) \sin \psi \qquad \eta_1 = \hat{\eta}_1 \sin \psi \qquad \xi_1 = \hat{\xi}_1 \cos \psi \qquad \zeta_1 = \hat{\zeta}_1 \sin \psi \quad (16)$$

the problem reduces to a system of linear ordinary differential equations (by omitting the $\hat{}$ sign):

$$\frac{du_1}{dy} + \frac{u_1}{y} - \frac{v_1}{y} - ikaw_1 = -(ikayw_0 + u_0) \tag{17}$$

$$\frac{d^2u_1}{dy^2} + \frac{1}{y}\frac{du_1}{dy} - \left(\frac{2}{y^2} + i\alpha^2\right)u_1 + \frac{2v_1}{y^2} - \frac{a}{\mu}\frac{dp_1}{dy} = -\left(\frac{du_0}{dy} + 2ika\,w_0 + 2\frac{\rho a \bar{w}_0}{\mu}\,w_0\right) \tag{18}$$

$$\frac{d^2v_1}{dy^2} + \frac{1}{y}\frac{dv_1}{dy} - \left(\frac{2}{y^2} + i\alpha^2\right)v_1 + \frac{2u_1}{y^2} - \frac{ap_1}{\mu y} = -\left(\frac{u_0}{y} + 2ikaw_0 + 2\frac{\rho a \bar{w}_0}{\mu}\,w_0\right) \tag{19}$$

$$\frac{d^2w_1}{dy^2} + \frac{1}{y}\frac{dw_1}{dy} - \left(\frac{1}{y^2} + i\alpha^2\right)w_1 + \frac{ika^2}{\mu}p_1 = -\left(\frac{dw_0}{dy} - \frac{ika^2y}{\mu}p_0\right) \tag{20}$$

$$\left(1 - \frac{\rho_t a^2\omega^2}{B}\right)\eta_1 - \xi_1 - ika\sigma\zeta_1 = \frac{a}{Bh}\left[ap_1 - 2\mu\frac{du_1}{dy}\right]_{y=1} - 2\sigma\eta_0 + ika(1-\sigma)\zeta_0 \tag{21}$$

$$-\left(1 + \frac{k^2a^2G}{B} - \frac{\rho_t a^2\omega^2}{B}\right)\xi_1 + \eta_1 - ika\left(\frac{G}{B} + \sigma\right)\zeta_1 = \frac{a\mu}{Bh}\left[u_1 + \frac{dv_1}{dy} - v_1\right]_{y=1}$$
$$-\eta_0 - ika\left(1 + \frac{G}{B}\right)\zeta_0 \tag{22}$$

$$-\left(\frac{G}{B} + k^2a^2 - \frac{\rho_t a^2\omega^2}{B}\right)\zeta_1 - ika\sigma\eta_1 + ika\left(\frac{G}{B} + \sigma\right)\xi_1 = \frac{a\mu}{Bh}\left[\frac{dw_1}{dy} - w_0\right]_{y=1}$$
$$-ika(\sigma - 1)\eta_0 - \left(\frac{G}{B} + 2k^2a^2\right)\zeta_0 \tag{23}$$

with $\alpha = a\sqrt{\dfrac{\rho\omega}{\mu}}$ the Womersley number. Because of the continuity of the physical variables in $y = 0$, the following boundary conditions are imposed in the origin:

$$u_1(0) = v_1(0) \qquad u_1'(0) = v_1'(0) = 0 \qquad p_1(0) = w_1(0) = 0 \tag{24}$$

and the fluid-wall matching velocity conditions are set at the wall (cfr. Eq. (14)):

$$i\omega\eta_1 = u_1(1) \qquad i\omega\xi_1 = v_1(1) \qquad i\omega\zeta_1 = w_1(1) \tag{25}$$

8

The fluid-structure interaction first order problem is similar to the zero-th order problem, but lack of geometrical symmetry makes the search of analytical solutions hard. Therefore the non homogeneous system is solved numerically. The flow Eqs. (17)–(20) are discretized in $[0,1]$ by upwind finite differences[17]. Coupled with the flow equations, the wall motion Eqs. (21)–(23) are solved together with the boundary conditions (24) in $y = 0$ and with the interface conditions (25) in $y = 1$. The resulting algebraic system is solved with an iterative procedure, using a preconditioner to stabilize the ill-conditioned problem.

5. Numerical results and discussion

Once the 0th order solution is obtained analytically and 1st order solution is computed, the full solution is then reassembled as:

$$\chi = \bar{\chi} + \tilde{\chi}e^{i(\omega t - kz)} = \bar{\chi} + |\tilde{\chi}| \cos\left(\omega t - \texttt{Re}(k)\,z + \phi\right)\exp(\texttt{Im}(k)\,z) \qquad (26)$$

with $\phi = \texttt{arg}(\tilde{\chi})$ (see Eq. (6)). It follows that all the variables have an oscillatory evolution in time, superimposed over the steady state solution, with amplitude $|\tilde{\chi}|$ and a phase lead or a phase lag ϕ. Both amplitude and phase are independent of time, while the amplitude has a damping factor given by $\texttt{exp}(\texttt{Im}(\texttt{k})z)$.

The physical problem depends on a large number of parameters, each of them may vary in a quite wide range, and there is an enormous variety of different limiting cases. In the present work we will focus the attention on the influence of curvature – parametrized by ε – letting all the others fixed.

In the simulations, we take the following numerical parameters, referred to the vascular flow in a medium sized arterial segment:

$$\omega = 2\pi\,s^{-1} \qquad a = 0.5\,cm \qquad h = 0.05\,cm \qquad E = 10^7\,dyne/cm^2$$
$$\mu = 0.04g\,cm^{-1}\,s^{-1} \qquad \rho = \rho_t = 1\,g/cm^3 \qquad \sigma = 0.5$$
$$A = 26000\,dyne/cm^2 \qquad \frac{d\bar{p}_0}{dz} = 7\,dyne/cm^3$$

The mesh size has been taken as $\Delta y = 0.02\,cm$.

A cross section of a curved tube with the inner wall at the left side is considered (Fig. 1). Eq. (26) is used to plot the flow pattern, the pressure distribution and wall deformations for a given time $(t = 0)$ and a fixed axial coordinate $(z = 0)$.

The effect of the curvature is examined by letting ε vary as $\varepsilon = 0, 0.05, 0.1$, and the correspondent amplitudes of the unsteady solution
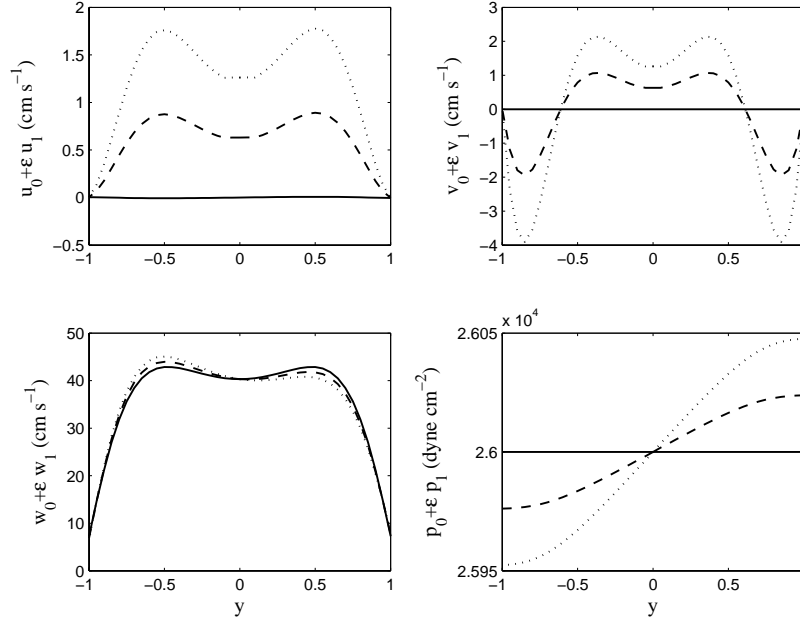
Figure 2.   Amplitude of the unsteady solution $\chi_0 + \varepsilon\hat{\chi}_1$ for $\varepsilon = 0$ (continuous line), $\varepsilon = 0.05$ (dashed line) and $\varepsilon = 0.1$ (dotted line) along $[-1, 1]$.

$\chi_0 + \varepsilon\hat{\chi}_1$ are depicted in Fig. 2. Note that in a curved tube the solution becomes asymmetric and the degree of skewness increases with ε. The structure and the evolution of the secondary flow is shown in Fig. 3. For the values of the parameters considered, a single vortex appears at most times, but a second vortex detaches from the wall and develops at the end of each half-cycle in the opposite direction. The strength of the secondary motion is measured through the index $\Sigma = \max\limits_{r,\psi} \sqrt{(\mathrm{Re}\tilde{u})^2 + (\mathrm{Re}\tilde{v})^2}$ (maximum modulus of the cross section velocity). Axial velocity peak is shifted alternately inwardly and outwardly, and a reversal flow takes place at some instants.

The amplitudes of the two components of the wall shear stress are obtained from the flow field as:

$$\tilde{\tau}_\psi = \tilde{\tau}_\psi^0 + \varepsilon\tilde{\tau}_\psi^1 = \varepsilon\tilde{\tau}_\psi^1 = \frac{\mu\varepsilon}{a}\left[\hat{u}_1 + \frac{d\hat{v}_1}{dy} - \hat{v}_1\right]_{y=1} \cos\psi \qquad (27)$$

$$\tilde{\tau}_z = \tilde{\tau}_z^0 + \varepsilon\tilde{\tau}_z^1 = \frac{\mu}{a}\left[\frac{d\tilde{w}_0}{dy} + \varepsilon\left(\frac{d\hat{w}_1}{dy} - \hat{w}_0\right)\sin\psi\right]_{y=1} \qquad (28)$$
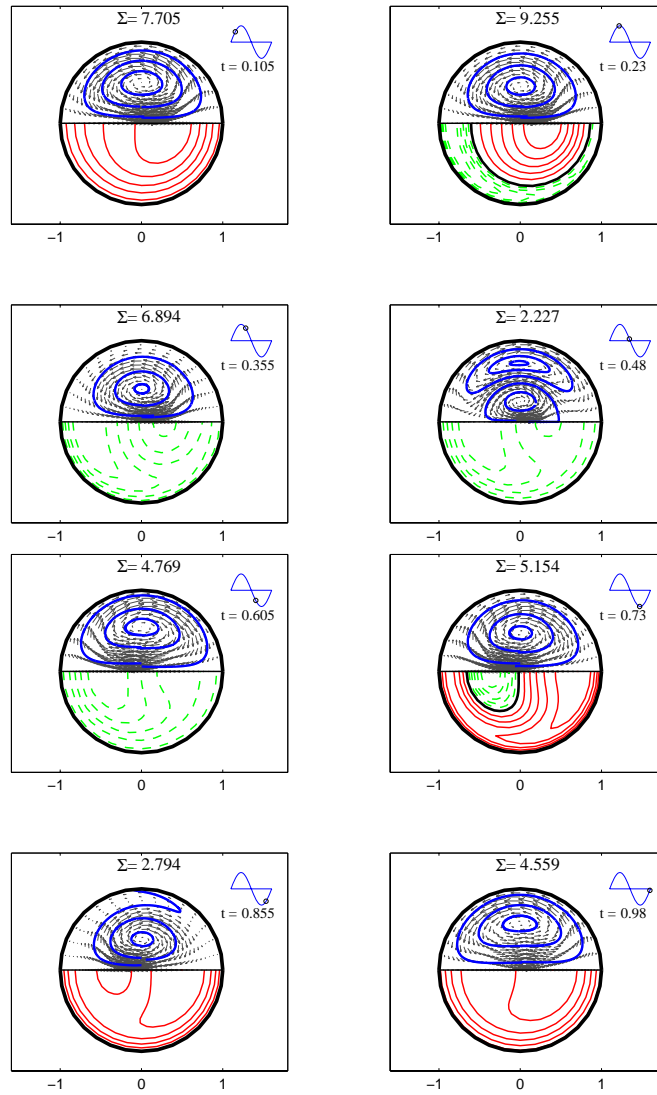
10

Figure 3.   Streamlines and secondary flow (above) and contour equispaced lines for axial velocity (below - continuous lines indicate positive levels, dashed lines negative levels, bold line zero levels) at eight times in a period at $z = 0$. The plot refers to the steady state solution summed up to unsteady solution $\bar{\chi} + \tilde{\chi}e^{i(\omega t - kz)}$, with $\varepsilon = 0.1$. A double vortex develops at the end of each half-cycle in correspondence of a small Σ.
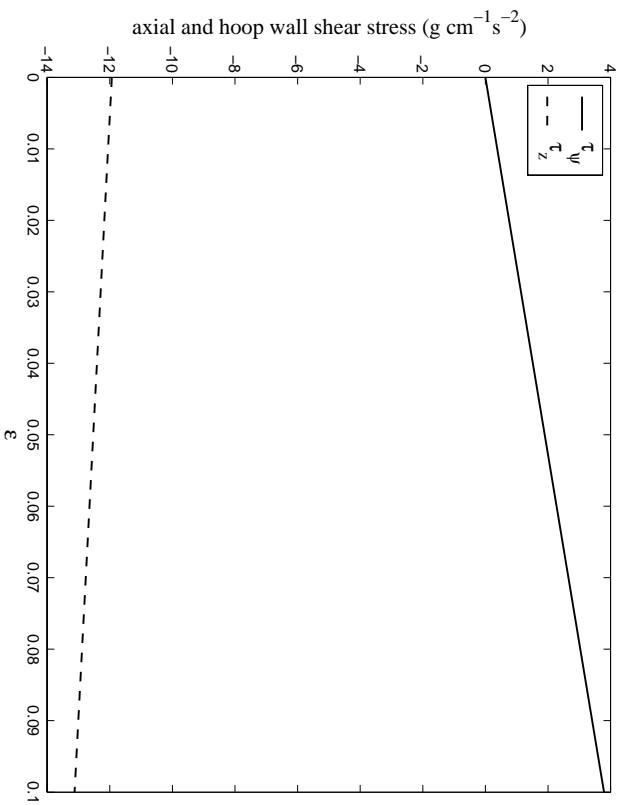
Figure 4. Amplitude at $t = 0, z = 0$ of the axial ($\tilde{\tau}z$) and hoop ($\tilde{\tau}_\psi$) wall shear stresses as functions of ε. The plots refer to the maximum values with respect to ψ.

From Eq. (27) it follows that the circumferential stress $\tilde{\tau}_\psi$ is present only in a curved tube and varies over a zero mean. On the other hand, the axial wall shear stress $\tilde{\tau}_z$ varies over the correspondent value for the straight tube $\tilde{\tau}_z^0$ and its extrema are attained at $\psi = \pm\frac{\pi}{2}$ (Eq. (28)). Both of them vary linearly with ε, are opposite in sign, and the magnitude of the $\tilde{\tau}_\psi$ is smaller than $\tilde{\tau}_z$ (Fig. 4).

Similarly to the flow variables, the wall displacements are trigonometric functions of ψ (see Eq.(16)): as consequence $|\tilde{\gamma}|$ and $|\tilde{\zeta}|$ are maximum at $\psi = \pm\frac{\pi}{2}$, while $|\tilde{\xi}|$ reaches its peaks at $\psi = 0$ and $\psi = \pi$, varying over their 0-th order mean. For a $E \lesssim 10^6$, the axial displacement amplitude becomes excessively large and this model is not consistent with the theory of linear elasticity and hence no longer representative.

For additional results and a more extensive discussion, see Ref. 15.

Acknowledgments

12

References

1. T.J. Pedley, *The fluid mechanics of large blood vessels*, **Chapt. 4**, Cambridge Univ. Press (1980).
2. S.A. Berger, L. Talbot and L.S. Tao, *Ann. Rev. Fluid Mech.*, **15**, 461 (1983).
3. W. R. Milnor, *Hemodynamics*, 2nd ed., Williams and Wilkins, **C8** (1989).
4. W.R. Dean, *Phil. Mag.*, **4**, 208 (1927).
5. W. H. Lyne, *J. Fluid. Mech.*, **45**, 13 (1970).
6. R. G. Zalosh and W.G. Nelson, *J. Fluid. Mech.*, **59**, 693 (1973).
7. T. Mullin and C. A. Greated, *J. Fluid. Mech.*, **98**, 397 (1980).
8. J.R. Womersley, *Phil. Mag.*, **46**, 199 (1955).
9. K. Sudo, M. Sumida and R. Yamane, *J. Fluid. Mech.*, **237**, 189 (1992).
10. F. T. Smith, *J. Fluid. Mech.*, **71**, 15 (1975).
11. D. M. Wang and J. M. Tarbell, *J. Biomech. Eng.*, **117**, 127 (1995).
12. L. J. Chang and J. M. Tarbell, *J. Fluid. Mech.*, **161**, 175 (1985).
13. K. B. Chandran, W. M. Swanson, D. N. Ghista and H. W. Yao, *Ann. Biomed. Eng.*, **2**, 392 (1974).
14. L.J. Myers and W.L. Capper, *IEEE Trans. Biomed. Engin.*, **48**, n. 8, 864 (2001).
15. G. Pontrelli and A. Tatone, *Euro J. Mech. (solids)*, submitted (2004).
16. Y.C. Fung, *A first course in continuum mechanics*, Prentice Hall Inc. (1977).
17. C.A.J. Fletcher, *Computational techniques for fluid dynamics*, Vol.I, Springer-Verlag (1997).